

Optimizing Bifacial Silicon Heterojunction Solar Cells for High-Latitudes

Erin M. Tonita, Amanda R. Lewis, Christopher E. Valdivia, and Karin Hinzer
SUNLAB, Centre for Research in Photonics, University of Ottawa, Ottawa, ON, Canada

Abstract— Two-dimensional optoelectronic modelling of bifacial silicon heterojunction solar cells is completed in Synopsys TCAD Sentaurus to optimize and characterize cell performance for regions of high latitude where cells experience high average air mass and increased angles of incidence. Cell performance under bifacial illumination conditions representative of the Canadian High Arctic, with independent spectra illuminating the front and rear faces of the cell, is studied. The baseline cell structure has an efficiency of 20.4% and 19.3% under front-face illumination with AM1.5G and AM3.0G, respectively. Improvements will be made through the addition of surface texturing and the optimization of doping, layer thicknesses, and antireflection coatings.

Keywords— bifacial solar cells, bifacial illumination, silicon heterojunction solar cells, high-latitude optoelectronic modelling.

I. INTRODUCTION

Silicon heterojunction (SHJ) solar cells made with thin-layered amorphous silicon currently hold the record for silicon solar cell efficiency [1], and can be adapted for bifacial applications with little added fabrication cost. While typically designed for areas with long sunshine duration and low-latitude, bifacial solar cells are also beneficial for high-latitude applications due to increased bifacial gain. Solar cells placed at higher latitudes will experience higher average air mass, increased diffuse lighting, and lower average temperatures. Additionally, the ground conditions around the solar cells will influence cell performance, with significant periods of the year being snow-covered. A numerical simulation modelling high latitude conditions for bifacial SHJ cells has been developed in Synopsys TCAD Sentaurus, allowing for characterization of cell performance under a variety of operating and illumination conditions.

II. SIMULATION

Bifacial SHJ solar cells are defined and discretized in two-dimensions in Sentaurus with thin-layered amorphous silicon on both sides of a monocrystalline wafer. A layer of indium tin oxide (ITO) is deposited on the top and the bottom of the cell, providing lateral charge transport and antireflection properties. Once the meshing strategy has been applied, material parameters are assigned to each region in the mesh. Optical and electrical material parameters for ITO, amorphous silicon, and crystalline silicon are taken from literature [2] and used as simulation inputs, apart from the complex index of refraction, which has been measured experimentally at Arizona State University. Figure 1 outlines the structure and layer thicknesses of the solar cell simulated in this work.

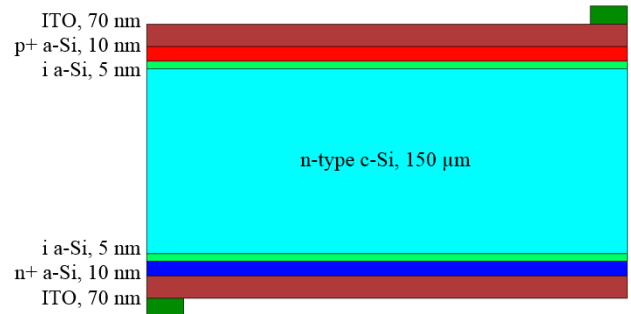


Figure 1. Schematic diagram of the bifacial SHJ structure modelled in this abstract.

The Transfer Matrix Method (TMM) is used to calculate the optical generation of carriers under varying illumination conditions. This calculation is done for a vertical cutline through the structure, resulting in a carrier generation profile that is then applied across the cell for regions where there is no contact shading. Optical carrier generation is solved for each wavelength over the incident light spectrum and summed. Once the carrier generation profile has been calculated for every region in the mesh, an electrical simulation follows. The electrostatic potential, ϕ , is given by Poisson's equation,

$$\nabla \cdot (\epsilon \nabla \phi) = q (p - n + N_D^+ - N_A^-), \quad (1)$$

with p and n being the electron and hole carrier concentrations, respectively, and N_D^+ and N_A^- the donor and acceptor ion concentrations. Equation (1) is first solved at equilibrium alongside the carrier continuity equations for electrons and holes,

$$\delta n / \delta t = (1/q) \nabla \cdot J_n + G_n - R_n = 0, \quad (2)$$

$$\delta p / \delta t = (-1/q) \nabla \cdot J_p + G_p - R_p = 0, \quad (3)$$

where J is the conduction current density, G corresponds to the generation rate of carriers, and R is the total recombination rate that results from Auger, Shockley-Read-Hall, radiative, and surface recombination. Non-equilibrium solutions are found by ramping incident light intensity. The electronic properties of the cell, including current-voltage behaviour, are calculated by solving the coupled drift-diffusion equations as the contact voltage across the cell is ramped. For example, Figure 2 demonstrates the simulated energy band diagram that results at the front-face intrinsic a-Si/c-Si interface during short-circuit operation. An additional simulation ramping incident wavelength is completed to calculate properties including reflection, absorption, and internal and external quantum efficiency. A similar solar cell modelling approach is described in detail in Reference [3].

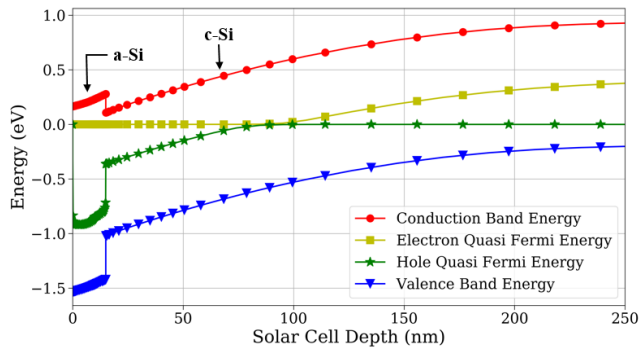


Figure 2. Energy band diagram for the front face of a bifacial SHJ solar cell operating at short-circuit current.

III. RESULTS

A bifacial illumination scheme has been developed in Sentaurus, utilizing two independent optical illumination windows for the front and rear faces of the cell. Simulations compare device performance under standard AM1.5G illumination to spectra of different air mass (e.g. AM3.0G). Figure 3 below demonstrates the simulated current-voltage curve of a front-face illuminated SHJ cell for spectra of different air mass. As expected, AM3.0G illumination results in a significant drop in short-circuit current compared to the standard AM1.5G illumination spectrum. The short-circuit current decreases from 32.2 mA/cm² to 21.1 mA/cm², a loss which can be accounted for due to the overall drop in incident light intensity as air mass index is increased. The efficiency also marginally decreases for increased air mass, as the spectrum of incident power changes.

Simulations are also done for rear-side illumination. Rear illumination spectra are albedo-modified for various surfaces [4], including snow and dry grass. For the present cell design, a 5% drop in maximum power point (MPP) under rear-face illumination occurs for both snow-modified AM1.5G and AM3.0G spectra, while rear-face MPP drops by 58% and 57% for dry grass-modified AM1.5G and AM3.0G, respectively. A bifacial illumination scheme is currently being developed in Sentaurus to compute cell performance when the front and rear faces of the cell are simultaneously illuminated with light of varying intensity.

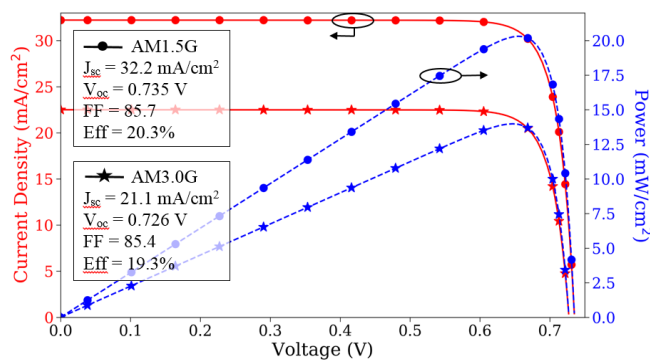


Figure 3. Simulation of IV and PV curves for a bifacial SHJ solar cell under front-face AM1.5G and AM3.0G illumination. Cell performance parameters are inset.

Quantum efficiency of the bifacial SHJ solar cell is found over the wavelength range of the incident light. Figure 4 depicts the cell's external quantum efficiency, defined as the number of carriers collected for each photon incident on the solar cell. The external quantum efficiency is limited in the near-infrared by rear-surface recombination and increased transmission for longer wavelengths, before being ultimately limited by the bandgap of the crystalline silicon substrate. The ultraviolet wavelength region is limited by surface recombination losses and by reflections that occur at the front surface. The external quantum efficiency can be improved by optimizing the antireflection coating of the cell. In the future, this will include the addition of surface texturing. The passivation quality of intrinsic amorphous silicon will also be explored in greater detail, in order to characterize and minimize surface recombination between the crystalline silicon and amorphous silicon layers.

IV. SUMMARY

Solar cell structure will first be optimized via the antireflection coating, surface texturing, doping, and layer thicknesses, for AM1.5G bifacial illumination before being optimized for higher air masses. By exploring the impact of changes in air mass, temperature, and lighting conditions, this optimization can also lead to a greater understanding of bifacial cell optimization at lower-latitudes. The results of bifacial optimization under high-latitude operating conditions will be presented, and will inform the fabrication and deployment of solar cells for testing in Cambridge Bay, Nunavut.

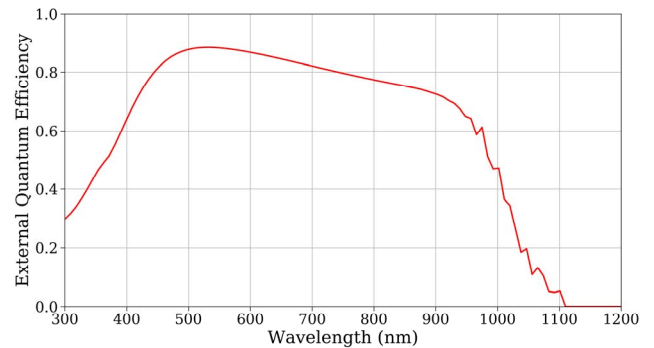


Figure 4. Simulation of external quantum efficiency for a bifacial SHJ solar cell.

REFERENCES

- [1]. K. Yoshikawa, et al., "Silicon heterojunction solar cell with interdigitated back contacts for a photoconversion efficiency over 26%", *Nature Energy*, 2(5), 17032 (2017).
- [2]. A. Fell, et al., "Input parameters for the simulation of silicon solar cells", *IEEE J. of Photovolt.*, 5 (4), 1250-1262 (2015).
- [3]. M. Wilkins and K. Hinzer, "Multijunction solar cells", in *Handbook of Optoelectronic Device Modeling and Simulations*, vol. 2, J. Piprek, Ed. Boca Raton: CRC Press, 2018, pp. 415-440.
- [4]. T. C. R. Russell, R. Saive, A. Augusto, S. G. Bowden, and H. A. Atwater, "The influence of spectral albedo on bifacial solar cells: a theoretical and experimental study", *IEEE J. of Photovolt.*, 7(6), 1611-1618 (2017).